Materials Today: Proceedings 38 (2021) 1018–1023

Contents lists available at ScienceDirect

Materials Today: Proceedings

journal homepage: www.elsevier.com/locate/matpr

# Numerical investigation of creep-fatigue interaction of straight P91 steam pipe subjected to start-up and shutdown cycles

Smith Salifu [a,*], Dawood Desai [a], Schalk Kok [b]

[a] Department of Mechanical and Automation Engineering, Tshwane University of Technology, Pretoria, South Africa
[b] Department of Mechanical and Aeronautical Engineering, University of Pretoria, Pretoria, South Africa

A R T I C L E I N F O

*Article history:*
Received 8 April 2020
Received in revised form 21 May 2020
Accepted 24 May 2020
Available online 18 June 2020

*Keywords:*
Creep
Creep-fatigue interaction
Start-up and shutdown cycle
Abaqus
fe-safe/Turbolife

A B S T R A C T

Components subjected to operation at a temperature in the range of 0.4 Tm (Melting temperature of component) and above are prone to failure due to creep. The failure becomes more severe when the component is further subjected to a sequence of start-up and shutdown cycles. If the cycles are enough to induce extensive plastic strain, the failure of the component could be attributed to a combined effect of creep and fatigue known as creep-fatigue interaction. In this paper, the creep-fatigue behaviour of a straight P91 (9Cr-1Mo) martensitic stainless steel steam pipe subjected to a 24 h daily sequence of start-up and shutdown cycles under a typical operating temperature of 550 °C and pressure of 18 MPa was investigated using finite element analysis code, Abaqus CAE/2019 in conjunction with fe-safe/Turbolife software. The outcome of the analysis shows that the failure of the steam pipe under the specified start-up and shutdown cycles is strictly due to creep since the operational cycle was insufficient to induce the required plastic strain capable of initiating fatigue failure. Nevertheless, the maximum creep stress developed in the pipe after an hour of operation is 126.6 MPa with a corresponding creep rate of $1.114 \times 10^{-7} h^{-1}$, while the creep stress and strain developed after 24 h operational cycle is 126.3 and $9.044 \times 10^{-7}$ respectively. Hence, the useful creep life and maximum creep damage for the machined-finished surface P91 steam pipe are 23.68 years and $4.823 \times 10^{-6}$ respectively. Lastly, a strong correlation was obtained between the analytically and numerically computed creep strain rates.

Selection and peer-review under responsibility of the scientific committee of the International Symposium on Nanostructured, Nanoengineered and Advanced Materials.

## 1. Introduction

The geometrical growth of the population of the earth and industries has resulted in consequential increase in the demand for electrical energy. To meet this demand, the power generation companies are left with no option other than to increase the operating parameters of their plants such as the temperature and pressure and also adjust the operating sequence to accommodate peak and off-peak periods of electrical energy demand. The operational routines of the power generation plants have consequential effect on the components of the plant such as the steam pipes, and the useful creep, fatigue and creep-fatigue life of the pipes are significantly affected [1]. Hence, components capable of withstanding the increment in operating parameters and maintain appreciable useful life during operation is required for use as a steam pipe. Thus, steam pipes are fabricated from martensitic stainless steels such as P91 (9Cr-1Mo) [2] on the account of the superior creep strength, high corrosion resistance [3] and excellent weldability [4–6] behaviour they display at high temperature. P91 steel is often used as headers in steam generators and tubing in the transportation of steam from the boiling compartment to the turbines. At elevated temperature, P91 steel displays high strength due to the complex microstructure it exhibits. This microstructure causes high dislocation density with lath and sub boundaries having M23C6 and MX type precipitates in the matrix. [6]. The inter-particle spacing of the MX type precipitates, good resistance to coarsening and increased volume fraction are some of the factors responsible for enhanced creep strength of P91 steel [6].

Despite the use of high strength steel as steam pipes, the unusual cycles consisting of several start-up phases closely followed by a steady or constant high temperature and pressure operation, then the shutdown phases [7] has significant influence on the useful life of the pipe as they are invariably subjected to operation in

* Corresponding author.
*E-mail address:* smithsalifu@gmail.com (S. Salifu).

https://doi.org/10.1016/j.matpr.2020.05.613
2214-7853/© 2019 Elsevier Ltd. All rights reserved.
Selection and peer-review under responsibility of the scientific committee of the International Symposium on Nanostructured, Nanoengineered and Advanced Materials.

creep-fatigue regime and failure due to creep-fatigue damage is presumed to be imminent [1]. Creep failure is a well-established failure mode in components subjected to elevated temperature operation. However, a more complicated failure mode due to creep-fatigue interaction is activated when the component is subjected to cyclic loading in addition to operating under elevated temperature [8].

Under creep-fatigue interaction, the accumulated damage rate under a complex loading differs from the summation of the linear rate of damages produced by components under creep and cyclic loading [1,9]. The microstructure of component subjected to creep-fatigue interaction condition depicts a combined effect emanating from creep damage and fatigue damage. The manifestation of fatigue failure is due to crack damage while creep failure is through the formation of creep voids on the interior grain boundaries. In the simultaneous presence of both termed creep-fatigue interaction, creep cavitation alongside surface fatigue damage are found within the material and this results in an accelerated failure with the failure path exhibiting a mixed trans and intergranular path.

Quite a number of research work has been done in a creep-fatigue environment targeted at determining the possibility of creep-fatigue interaction occurring [8,10–12], however, there is still profuse controversies as regard this failure mode in steam pipes as the start-up and shutdown cycles in power generation plants is presumed be insufficient to induce failure due to fatigue [13]. In order to determine the possibility of creep-fatigue interaction occurring in a component, time fraction rule recommended by the prevailing standard such as RCC-MR [14] and ASME BPVC [15] is used while R5 uses the ductility exhaustion approach [16]. The structural integrity of an elevated temperature component is guaranteed if the damage evolution is well understood, particularly the interaction damage in a creep-fatigue environment [17,18].

In this paper, finite analysis code, Abaqus in conjunction with fe-safe/Turbolife software was used to determine the creep behaviour and the possibility of creep-fatigue failure occurring in a straight P91 (9Cr-1Mo-V) steam pipe subjected to a 24 h daily start-up and shutdown cycles. The creep behaviour was determined using Abaqus CAE/2019 while the possibility of creep-fatigue interaction occurring due to the operational start-up and shutdown cycles was investigated using the R5 standard ductility method in fe-safe/Turbolife software.

## 2. Thermo-mechanical stress model developed in a straight pipe

A thick-walled pipe subjected to internal pressure, P, generates three principal stresses. These stresses are hoop or circumferential$\sigma_t$, radial$\sigma_r$ and axial or longitudinal stress$\sigma_z$. The head of the pipe is responsible for the axial stress developed and the value of this stress is constant throughout the analysis while the two other stresses vary throughout the pipe [19]. The expressions for the three stresses developed in a thick piped with external and internal radii $r_o$ and $r_i$wasintroducedby Lamé [20] as shown in Eq. (1)-(3).

$$\sigma_r = P\frac{r_i^2\left(r^2 - r_o^2\right)}{r^2\left(r_o^2 - r_i^2\right)} \tag{1}$$

$$\sigma_t = P\frac{r_i^2\left(r^2 + r_o^2\right)}{r^2\left(r_o^2 - r_i^2\right)} \tag{2}$$

$$\sigma_z = \frac{P_i r_i^2}{r_o^2 - r_i^2} \tag{3}$$

The effective or total mechanical stress, $\sigma_{vm}$ developed in the pipe can be obtained using von-Mises theory as expressed in Eq 4.

$$\sigma_{vm} = \sqrt{\left[\sigma_t^2 + \sigma_r^2 + \sigma_z^2 - (\sigma_t\sigma_r + \sigma_t\sigma_z + \sigma_r\sigma_z)\right]} \tag{4}$$

Also, the thermal stress developed in a thick-walled pipe at elevated [21,22], can be expressed as follow:

$$\sigma_{tT} = \frac{\alpha E}{(1-v)r^2}\left[\frac{r^2 + r_i^2}{r_o^2 - r_i^2}\int_{r_i}^{r_o} Trdr - \int_{r_i}^{r} Trdr - Tr^2\right] \tag{5}$$

$$\sigma_{rT} = \frac{\alpha E}{(1-v)r^2}\left[\frac{r^2 - r_i^2}{r_o^2 - r_i^2}\int_{r_i}^{r_o} Trdr - \int_{r_i}^{r} Trdr\right] \tag{6}$$

$$\sigma_{zT} = \frac{\alpha E}{(1-v)}\left[\frac{2}{r_o^2 - r_i^2}\int_{r_i}^{r_o} Trdr - T\right] \tag{7}$$

Using von-Mises theory, the effective thermal stress is determined.

$$\sigma_{vmT} = \sqrt{\left[\sigma_{tT}^2 + \sigma_{rT}^2 + \sigma_{zT}^2 - (\sigma_{tT}\sigma_{rT} + \sigma_{tT}\sigma_{zT} + \sigma_{rT}\sigma_{zT})\right]} \tag{8}$$

where, $\sigma_r$,$\sigma_t$ and $\sigma_z$ represent radial, circumferential and axial mechanical stress respectively while $\sigma_{rT}$, $\sigma_{tT}$ and $\sigma_{zT}$ represent radial, circumferential and axial thermal stress respectively. The effective von-Mises mechanical and thermal stress is represented by $\sigma_{vm}$ and $\sigma_{vmT}$ is effective thermal von-Mises stress.

Hence, the thermo-mechanical stress, $\sigma_{TM}$ developed in a straight pipe subjected simultaneously to operation in a thermal and mechanical environment is determined by the summation of the effective mechanical and thermal stresses.

$$\sigma_{TM} = \sigma_{vm} + \sigma_{vmT} \tag{9}$$

### 2.1. Creep-fatigue interaction model

#### 2.1.1. Modified hyperbolic sine creep model

Under creep conditions, Garofalo [23,24] proposed an expression for creep strain rate capable of describing the creep rate of materials over a whole range of stress. The same expression, modified hyperbolic sine creep law under hot deformation condition was proposed by Sellar and Tegart [24]. The modified hyperbolic sine creep law, capable of capturing both high and low-stress regime can be express as

$$\dot{\varepsilon}_{cr} = A[\sinh(\sigma\beta)]^n\left[\frac{-Q}{RT}\right] \tag{10}$$

where A, n and $\beta$ are material constants, Q is activation energy, T is temperature and R is gas constant.

#### 2.1.2. Creep damage model

According to Ductility Exhaustion theory, the local strain experienced in a component subjected to operation in a creep regime attains critical ductility where there is forward propagation of a crack [18,25], and the rate of creep strain damage or strain rate damage can be obtained as shown in Eq. 11.

$$d_c = \frac{\varepsilon_c}{\varepsilon_f^*} \tag{11}$$

where $d_c$, $\varepsilon_c$ and $\varepsilon_f^*$ are the creep damage rate, creep strain rate and the multiaxial creep failure strain respectively.

### 2.2. Fatigue damage model

Based on the thermodynamic principle [1,26], low cycle fatigue can be calculated using the expression

$$\frac{d_f}{dN} = \frac{R_v}{\varphi(\gamma+1)}\frac{(\Delta p)^{\gamma+1}}{(1-\omega)^{\alpha_0}} \tag{12}$$

where, $\gamma$, $\varphi$ and $\alpha_0$ are material constants, $R_v$ represents stress triaxiality effect, $d_f$ is fatigue damage, $\Delta p$ is the accumulated plastic strain in one complete cycle. This can be obtained using the Ramberg-Osgood equation [8,27]:

$$\frac{\Delta\sigma_e}{2} = K'\left(\frac{\Delta p}{2}\right)^{n'} \tag{13}$$

where, $\Delta\sigma_e$ is the equivalent stress variation in one complete cycle and $n'$ and $K'$ are material constants.

### 2.3. Creep-fatigue interaction

A creep-fatigue interaction term that helps to determine the damage caused in a creep-fatigue environment was proposed by Lagneborg [28], and defined as:

$$d_{cf} = b((d_f/dN)(d_c/dN))^{1/2} \tag{14}$$

where, $d_{cf}$ is the damage due to creep-fatigue interaction, b is the coefficient of creep-fatigue interaction, which is a function of loading conditions, hold time, temperature, etc.

The $d_f/dN$ term represents the fatigue damage obtained in one complete cycle as expressed in Eq (11) while the term $d_c/dN$ represents the creep damage accumulated in one complete cycle. The accumulated creep damage shown in Eq. (10) can be expressed as

$$\frac{d_c}{dN} = \int_0^{t_h} d_c dt \tag{15}$$

where, $t_h$ represents the hold time in one complete cycle.

Hence, the creep-fatigue interaction damage model [1] can be expressed as

$$\frac{d_{cf}}{dN} = \frac{d_c}{dN} + \frac{d_f}{dN} + b\left(\left(\frac{d_c}{dN}\right)\left(\frac{d_f}{dN}\right)\right)^{1/2} \tag{15}$$

## 3. FE model

In order to replicate a real case scenario that captures the detailed behaviour of creep and possible creep-fatigue interaction in a straight power generation steam pipe during operation, a three-dimensional (3D) model of P91 steel pipe and pyrogel insulation jacket were developed in finite element analysis code, Abaqus CAE/2019 as shown in Fig. 1.

The dimension of the pipe and pyrogel insulation jacket used for the analysis are shown in Table 1. Global seed or mesh size of 20 mm with a total of 92 196 DC3D8 and 92 196 C3D8R element type for heat transfer and the creep/creep-fatigue analysis respectively was used for the simulation after conducting mesh convergence studies. On the inner surface of the pipe-insulation assembly, a sink temperature (operating temperature) of 550 °C with a corresponding film coefficient of 10 000 W/m²K was applied while on the outer surface of the assembly, a sink temperature (room temperature) of 25°Cwith a corresponding convective heat transfer coefficient of 18 W/m²K was applied [29]. Operating pressure of 18 MPa was applied to the inner surface of the assembly and an appropriate displacement/rotation mechanical boundary conditions were applied to both ends of the pipe-insulation as shown in Fig. 1(c).

The elastic and thermal material properties of P91 steel [31] with Poisson's ratio 0.33 and thermal conductivity of 33 W/mK are depicted in Figs. 2-3(a), and the uniaxial creep constants for the modified hyperbolic sine creep model shown in Table 2. was obtained through curve fitting of uniaxial creep test data conducted at 550 °C [32] and implemented via Fortran creep user subroutine script in Abaqus. The ultimate tensile strength of the steel is 585 MPa and its yield strength is 357.49 MPa at 550 °C [33]. To determine the creep damage and the possibility of creep-fatigue interaction occurring, Neuber plasticity method with elastic follow-up factor of 0.33, ductility exhaustion and Morrow correction algorithm [13] was implemented in fe-safe/Turbolife with the pipe assumed to have a machined-finished surface (16 < Ra <= 40um). A 24 h real case scenario having a total of 6 h peak period steady-state operation, 4 h transient state and 14 h off-peak steady-state downtime period as shown in Fig. 3(b) was implemented in this analysis.

## 4. Results and discussions

The graph for the mesh convergence study conducted and the meshed pipe-insulation assembly depicted in Fig. 4. (a) and (b) show that a total of 110 100 linear hexahedral elements type C3D8R with 149 609 nodes is suitable for the creep analysis while 110 100 linear hexahedral elements type DC3D8 with 149 609 nodes is suitable for the heat transfer analysis.

The temperature distribution profile contour plot displayed in Fig. 5(a) shows that the maximum operating temperature (550 °C) was maintained in the pipe during peak period of operation and the minimum value of temperature (35.37 °C) obtained on the outer surface of insulation jacket shows that pyrogel is a suitable insulation jacket for steam pipes [29].

The plot for the creep stress and strain rate developed in the pipe during the first one hour of peak period operation is shown in Fig. 5(b) while the creep stress and strain after 24 h complete cycle are shown in Fig. 6. After an hour of operation at peak period, a maximum creep stress of 126.5 MPa with a corresponding creep strain rate of $1.114 \times 10^{-7} h^{-1}$ was developed in the pipe-insulation assembly as shown in Fig. 5(b). The value of the creep stress was observed to relax to 126.3 MPa after 24 h complete cycle while the creep strain developed in after the same cycle as shown in Fig. 6 is $9.044 \times 10^{-7}$. It was observed that plastic strain was not

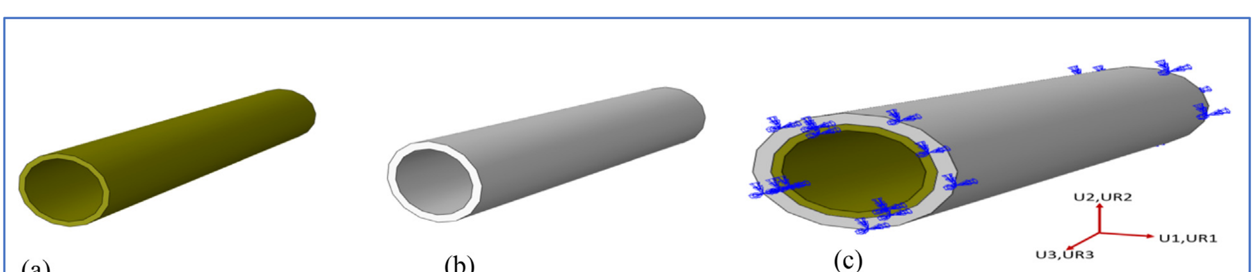


**Fig. 1.** Model of (a) P91 steel pipe, (b) pyrogel insulation jacket and (c) pipe-insulation jacket assembly with boundary condition.

**Table 1**
Dimensions of pyrogel insulation jacket [29,30]

| P91 steel pipe | | | Pyrogel insulation jacket | | |
|---|---|---|---|---|---|
| Length (m) | Internal diameter (m) | External diameter (m) | Length (m) | Internal diameter (m) | External diameter (m) |
| 1.0 | 0.38 | 0.44 | 1.0 | 0.44 | 0.54 |

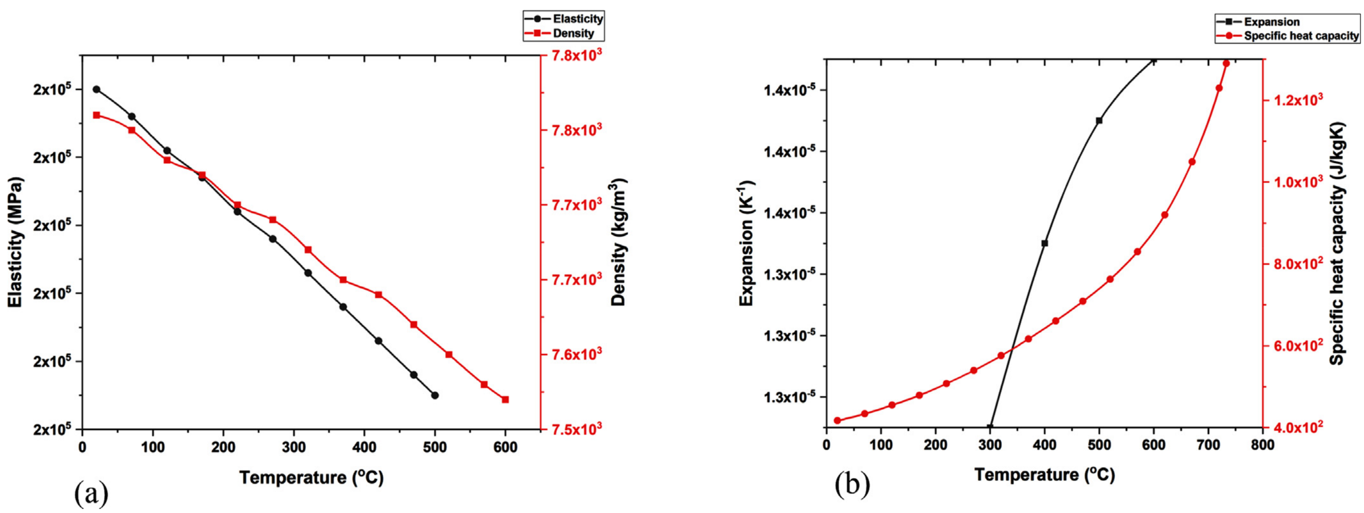


**Fig. 2.** (a) Elasticity and density, and (b) thermal expansion and specific heat capacity of P91 steel as a function of temperature.

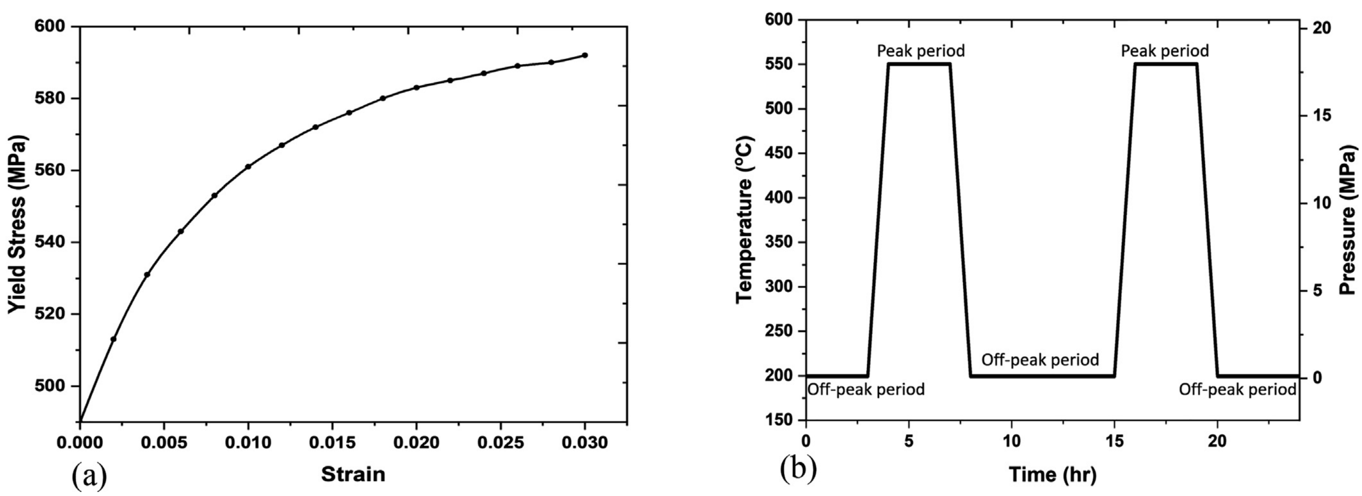


**Fig. 3.** (a) Plasticity of P91 steel and (b) 24 h start-up and shutdown operational cycle.

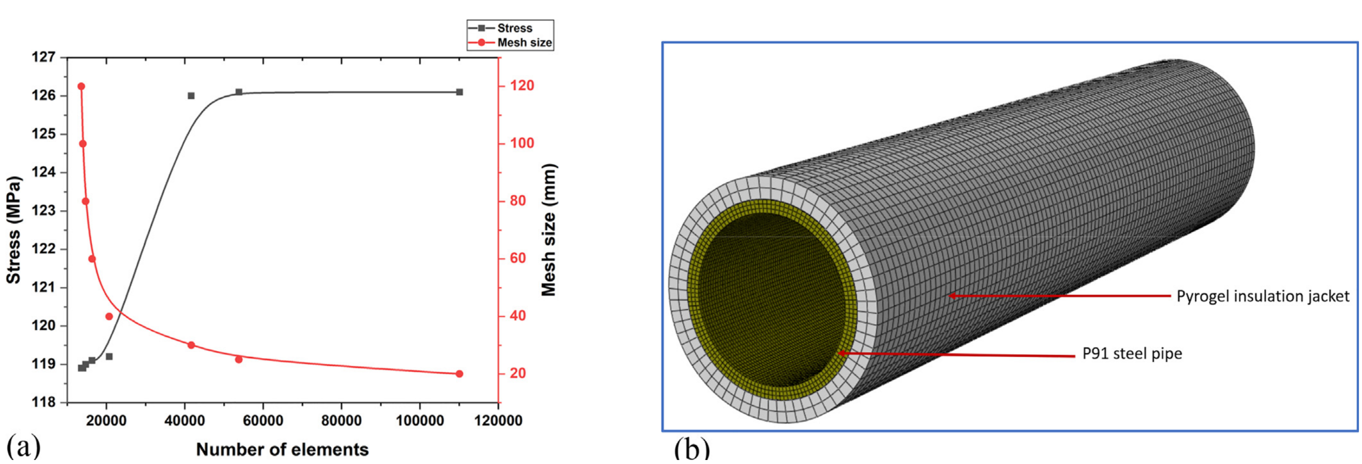


**Fig. 4.** (a) Mesh convergence study graph and (b) pipe-insulation jacket assembly mesh.

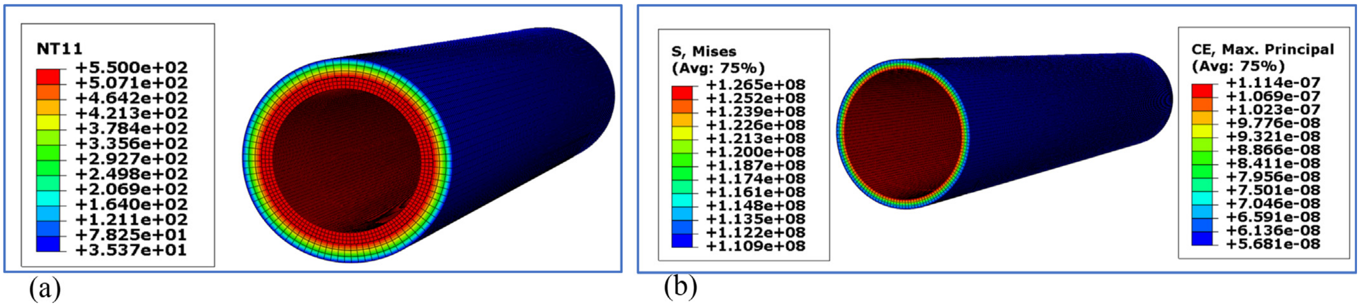


**Fig. 5.** Contour plot for (a) temperature distribution profile on the pipe-insulation assembly and (b) stress and creep strain rate distribution profile of P91 steam pipe after one-hour steady-state peak operation.

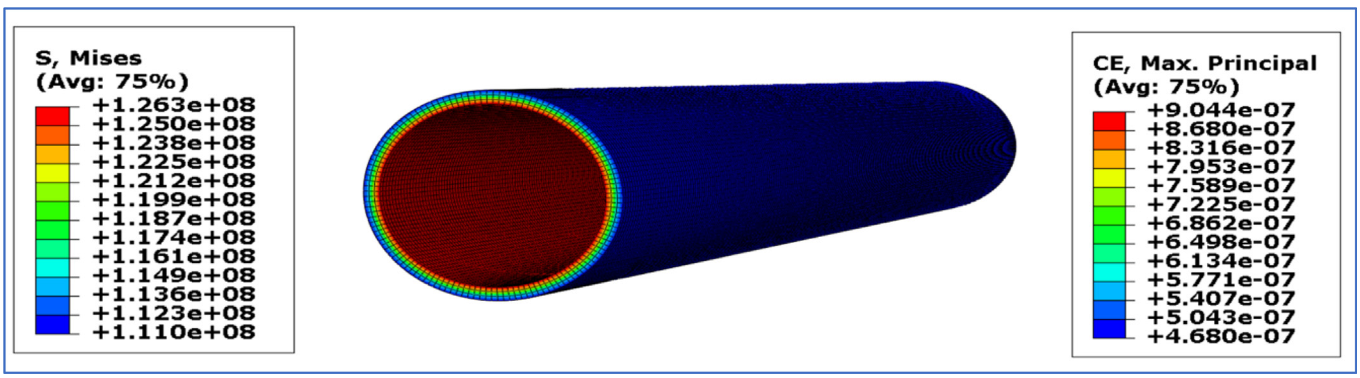


**Fig. 6.** Contour plot of stress and creep strain distribution profile after 24 h start-up and shutdown cycle.

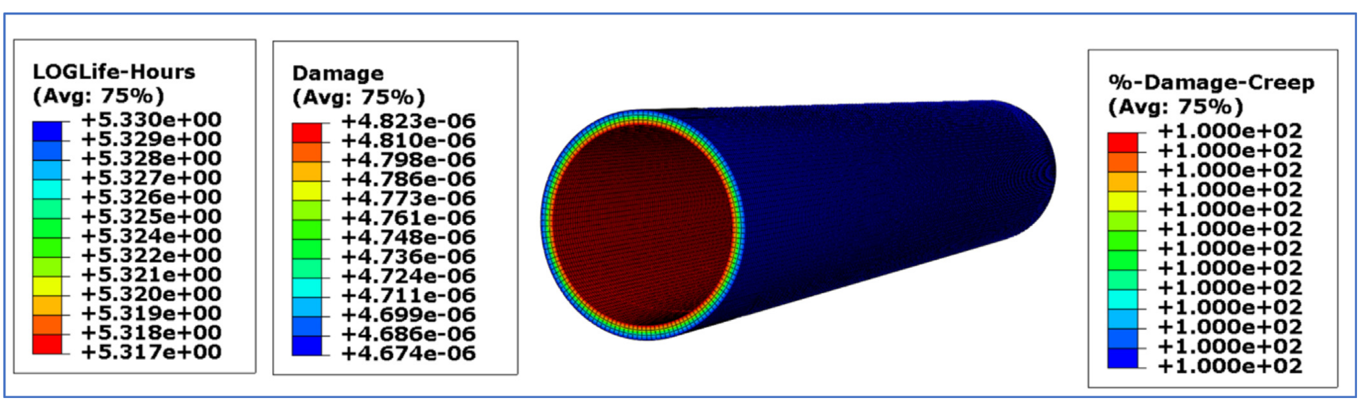


**Fig. 7.** Contour plot for creep life, damage and percentage creep damage due to the start-up and shutdown operational cycles.

**Table 2**
Modified hyperbolic sine creep constant for P91 steel at 550 °C [32].

| A<br>[ x $10^{29}h^{-1}$] | $\beta$<br>[ x $10^{-8}$ Pa] | n | Q<br>[J/(molK)] | R<br>[J/mol] | T<br>[K] |
|---|---|---|---|---|---|
| 3.50 | 2.37 | 1.32 | 599 342.4 | 8.314 | 823 |

developed in steam pipe regardless of the daily start-up and shutdown cycles it was subjected to.

The contour plot for the creep-fatigue analysis carried out with fe-safe/Turbolife software as depicted in Fig. 7. shows that the failure of the steam pipe under the specified daily operational cycle is strictly due to creep only. This is because the operational cycle was not enough to induce the plastic strain required for the initiation and propagation of fatigue failure. The LOGlife result shows that the steam pipe will survive 23.68 years prior to failure due to creep, and with a maximum damage of $4.823 \times 10^{-6}$.

### 4.1. Analytical validation

Using the equations for the thermo-mechanical stress developed in a thick-walled pipe, Eq. (1)-(9) and the expression for

**Table 3**
Comparison of analytical and simulated creep rate of the steam pipe after 1 h steady state peak operation.

| Analytical Stress [MPa] | Simulated Stress [MPa] | Analytical Creep Rate [$h^{-1}$] | Simulated Creep Rate [$h^{-1}$] | % Deviation in Creep rate |
|---|---|---|---|---|
| 126.78 | 126.5 | $1.120\times10^{-7}$ | $1.114\times10^{-7}$ | 0.54 |

the modified hyperbolic sine creep law, Eq. 10, the creep strain rate developed in the pipe after 1 h of steady-state peak operation was analytically validated. A strong correlation was obtained between the analytically calculated and numerically computed creep rate. The result of the comparison of both rates is shown in Table 3.

## 5. Conclusions

The possibility of straight P91 steam pipe subjected to a 24 h daily start-up and shutdown cycles characterized by a total of 6 h steady state peak period, 4 h transient period and 14 h steady-state off-peak period failing due to creep-fatigue interaction was investigated using finite element analysis code, Abaqus in conjunction with fe-safeTurbolife software. The main outcomes of this study are:

- The maximum operating temperature was maintained inside pipe during peak period operation while the temperature on the outer surface of the insulation jacket is 35.37 °C. This low value of temperature on the outer surface of the jacket is an affirmation that pyrogel is a good insulating jacket for steam pipes.
- The failure of the steam pipe under the stipulated operating conditions is strictly due to creep, and without fatigue or creep interacting with fatigue since the operating cycle was not enough to induce the required plastic strain that will initiate fatigue failure.
- It was further observed that the pipe will only survive 23.68 years under the stipulated operating condition prior to failure due to creep.
- Lastly, there is a strong agreement between the analytically calculated and numerically computed creep rate of the steam pipe.

## CRediT authorship contribution statement

**Smith Salifu:** Methodology, Writing - original draft, Validation. **Dawood Desai:** . **Schalk Kok:** Supervision.

## Declaration of Competing Interest

The authors declare that they have no known competing financial interests or personal relationships that could have appeared to influence the work reported in this paper.

## Acknowledgement

This research has been proudly supported by Tshwane University of Technology and the University of Pretoria, South Africa. Also, the authors greatly appreciate the unending support of Eskom Power Plant Engineering Institute (Republic of South Africa).

## References

[1] X. Zhang, T. Shan-Tung, F. Xuan, J. Theor. Appl. Fract. Mec. 71 (2014) 51–66.
[2] Z.F. Hu-F. J. T. P. P. (2012)195-226.
[3] Bharasi, N.S, K Thyagarajan, H Shaikh, M Radhika, A.K Balamurugan, S Venugopal, A Moitra, S Kalavathy, S Chandramouli, A.K Tyagi, R.K Dayal, J. Metall Mater Trans A., 43(2012) 561-571.
[4] P. Bocquet, P. Bourges, A. Cheviet, J. Nucl Eng Des. 144 (1993) 149–154.
[5] M. Sireesha, S. Sundaresan, S. Albert, J. Mater. Eng. Perform. 10 (2001) 320–330.
[6] K. Mariappan, V. Shankar, A.K. Bhaduri, Mater. High Temp. 39 (2020) 114–128.
[7] V. Shlyannikov, V. Tumanov, N. Boychenko, A creep stress intensity factor approach to creep–fatigue crack growth, J. Eng. Fract. Mech 142 (2015) (2015) 201–219.
[8] H. Jing, D. Su D, L. Xu, L. Zhao, Y. Han. Int. J, Fatigue 98(2017) 41-52.
[9] R. Hales, Fatigue Frac. Eng. M 3 (1980) 339–356.
[10] K. Sadananda, P. Shahinian, Metall. Mater. Trans A 11 (1980) 267–276.
[11] J. Wen, T. Tu, X. Gao, J. Reddy, J. Eng. Fract. Mech 98 (2013) 169–184.
[12] B. Fournier, M. Sauzay, C. Caës, M. Noblecourt, M. Mottot, A. Bougault, V. Rabeau, A. Pineau, Int. J. Fatigue 30 (2008) 649–662.
[13] Simulia Dassault Systemes, Providence, RI, fe-safe/TURBOlife user manual (2017)
[14] RCC-MRx Code, Design and Construction Rules for Mechanical Components of FBR Nuclear Islands and High Temperature Applications, Appendix A16 Tome I, vol (2007).
[15] American Society of Mechanical Engineers, Rules for Construction of Pressure vessels, Boiler ASEM, (2013).
[16] R. Ainsworth, R5: Assessment procedure for the high temperature response of structures, British Energy Generation Ltd 3 (2003).
[17] M. Chrzanowski, Int. J. Mech. Sci. 18 (1976) 69–73.
[18] L. Xu, L. Zhao, Z. Gao, Y. Han, Int. J. Mech. Sci. 130 (2017) 143–153.
[19] D. Annaratone, Cylinders under internal pressure, Press. Vessel. Des 2007 (2007) 47–127.
[20] B. Kanlıkama, A. Abuşoğlu, I.H. Güzelbey, Int. J. Energy. Power. Engr. 2 (2013) 60–68.
[21] A. Kandil, A. El-Kady, A. El-Kafrawy, Int. J. Mech. Sci. 37 (1995) 721–732.
[22] V. Pesonen. Online Creep and Fatigue Monitoring in Power Plants (2014).
[23] F. Garofalo, J. Trans. Metall. 227 (1963) 351–355.
[24] J.M. Montes, F.G. Cuevas, J. Cintas, J. Mater. Sci. Technol. 28 (2012) 377–379.
[25] R. Skelton, D. Gandy, Mater. High Temp. 25 (2008) 27–54.
[26] L. Lemaitre, J Eng Mater-T. 101 (1979) 284–292.
[27] W. Ramberg and W. R. Osgood. Description of stress-strain curves by three parameters. (1943).
[28] R. Lagneborg, R. Attermo, Metall. Mater. Trans. A 2 (1971) 1821–1827.
[29] S. Salifu, D. Desai, S. Kok, O. Ogunbiyi, Procedia Manuf. 35 (2019) 1330–1336.
[30] Pyrogel-XTE-Datasheet, High-Performance Aerogel Insulation for Industrial and Commercial Applications.
[31] JAHM Software. Temperature Dependent Material Properties Database. MPDB, " vol. MPDB vs8.77. (2020).
[32] Y. Gorash, D. MacKenzie, Open Eng. 7 (2017) 126–140.
[33] A. Zieliński, J. Dobrzański, Arch. Mater. Sci. Eng. 60 (2013) 72–81.